Microchimica Acta (2021) 188: 105
https://doi.org/10.1007/s00604-021-04762-9

ORIGINAL PAPER

Electrochemical immunosensor with Cu_2O nanocube coating for detection of SARS-CoV-2 spike protein

Zeinab Rahmati[1] · Mahmoud Roushani[1] · Hadi Hosseini[1] · Hamzeh Choobin[2]

Received: 4 November 2020 / Accepted: 16 February 2021 / Published online: 2 March 2021

Abstract

Severe acute respiratory syndrome SARS-CoV-2 has caused a global pandemic starting in 2020. Accordingly, testing is crucial for mitigating the economic and public health effects. In order to facilitate point-of-care diagnosis, this study aims at presenting a label-free electrochemical biosensor as a powerful nanobiodevice for SARS-CoV-2 spike protein detection. Utilizing the IgG anti-SARS-CoV-2 spike antibody onto the electrode surface as a specific platform in an ordered orientation through staphylococcal protein A (ProtA) is highly significant in fabricating the designed nanobiodevice. In this sense, the screen-printed carbon electrode modified with Cu_2O nanocubes (Cu_2O NCs), which provide a large surface area in a very small space, was applied in order to increase the ProtA loading on the electrode surface. Accordingly, the sensitivity and stability of the sensing platform significantly increased. The electrochemical evaluations proved that there is a very good linear relationship between the charge transfer resistance (R_{ct}) and spike protein contents via a specific binding reaction in the range 0.25 fg mL^{-1} to 1 μg mL^{-1}. Moreover, the assay when tested with influenza viruses 1 and 2 was performed in 20 min with a low detection limit of 0.04 fg mL^{-1} for spike protein without any cross-reactivity. The designed nanobiodevice exhibited an average satisfactory recovery rate of ~ 97–103% in different artificial sample matrices, i.e., saliva, artificial nasal, and universal transport medium (UTM), illustrating its high detection performance and practicability. The nanobiodevice was also tested using real patients and healthy samples, where the results had been already obtained using the standard polymerase chain reaction (PCR) procedure, and showed satisfactory results.

Keywords COVID-19 · Coronavirus · SARS-CoV-2 · Spike protein · Screen-printed carbon electrode · Cu_2O nanocubes · Nanobiodevice

Introduction

As a novel human infectious disease, coronavirus disease 2019 (COVID-19) which has been associated with severe respiratory distress was subsequently renamed as severe acute respiratory syndrome coronavirus 2 (SARS-CoV-2) by the International Committee of the Taxonomy of Viruses due to its similar symptom to SARS [1]. Previously, other types of CoV have been discovered [2]. However, it is worth mentioning that SARS-CoV-2 is much more contagious [3, 4]. The spread of this disease has not only led to the main health challenge in the world, but also has become an unprecedented socioeconomic burden [5]. As a result, the world increasingly needs diagnostic tools with the capability of identifying the infected individuals, e.g., the source of infection. In addition, infected people can be treated and isolated by effective diagnostics which result in slowing or stopping the spread of the infectious diseases.

When the coronavirus genetic code was published in early January, polymerase chain reaction–based experiments were widely performed around the world [6–8]. However, there are some specific limitations such as a relatively long detection time from 4 h up to 3 days, complicated sample pretreatment steps which can affect diagnostic accuracy, expensive equipment, and high cost [9]. Furthermore, performed in centralized diagnostic services by skilled personnel, PCR tests, despite their high sensitivity, are more suitable for the final

✉ Mahmoud Roushani
m.roushani@ilam.ac.ir; mahmoudroushani@yahoo.com

[1] Department of Chemistry, Faculty of Sciences, Ilam University, P. O. BOX. 69315-516, Ilam, Iran

[2] Department of Virology, Faculty of Medical Sciences, Tarbiat Modares University, Tehran, Iran

verification and not recommended for rapid screening and point-of-care testing. Moreover, when universal and low-cost point-of-care tools for the screening and early detection of diseases are provided, more population would access the healthcare services especially in remote areas [10–12]. Hence, in order to rapidly and accurately diagnose SARS-CoV-2, sensitive and inexpensive immunological diagnostic methods which aim at detecting viral antigens in clinical samples without sample preparation steps are necessary.

Nowadays, the biosensors allow sensitive and selective detection of a range of analytes due to their coupling with high-affinity biomolecules. Accordingly, they have received a lot of attention in the field of medical diagnosis as well as in a wide range of other fields such as point-of-care monitoring of treatment and disease progression, food control, drug discovery, environmental monitoring, forensics, and biomedical research [13–17]. In this regard, the immunosensors have been reported for virus detection using different transducers as better alternative to traditional assays. For instance, the detection of SARS-CoV-2 in universal transport medium (UTM) was done by graphene-based field-effect transistor, functionalized with SARS-CoV-2 spike antibody [18]. The label-free electrochemical sensor applying a commercially available impedance sensing platform, using specialized well plates which have integrated sensing electrodes from ACEA Biosciences, was also developed for the detection of SARS-CoV-2 antibodies [19]. The electrochemical assay was developed for spike protein or nucleocapsid protein detection using magnetic beads as support of immunological chain and secondary antibody with alkaline phosphatase as immunological label. This work was based on the detection of enzymatic by-product 1-naphtol using screen-printed electrodes modified with carbon black nanomaterial [20]. Another electrochemical sensor was developed for rapid detection of SARS-CoV-2 based on cobalt-functionalized TiO_2 nanotubes through sensing the spike (receptor-binding domain) present on the surface of the virus [21]. Thus, it is certain that immunosensor technology has an important place in the literature in terms of sensitive and selective biosensor design and analytical application.

Among the different biosensors, the electrochemical biosensors can be regarded as an important sensing method in the field of sensors [22]. As an effective immunoassay platform for quantitative, sensitive, and accurate detection, electrochemical immunosensor can include the advantages of electrochemical procedures, specific immunorecognition reaction, and biosensor devices. In addition, it possesses some other advantages, i.e., high sensitivity, low sensing expenses, fast response times, ease of use, small sample consumption, amenability to miniaturization, and subsequent portability, which result in giving it a significant potential for bedside testing (point-of-care) [23–25]. Accordingly, it becomes an appealing choice and holds great prospective as the next-generation detection strategy. Moreover, among the various electrodes which can be used as a platform in these sensors, screen-printed carbon electrode (SPCE) can provide an inexpensive kit and disposable devices for simple and rapid detection [26–29]. In order to enhance the performance characteristics of the biosensor and efficiently immobilize the biological molecules on the electrode surfaces, different nanomaterials have been used [30, 31]. Herein, in order to modify the electrode surface, we used Cu_2O nanocubes (NCs) which were prepared through a simple method by adding $CuCl_2$, NaOH, and ascorbic acid to aqueous solution. The Cu_2O NCs are well-known nanomaterials due to several benefits, including, low toxicity, availability, simple and cost-effective production method, strong adsorption ability, and large specific surface area [32, 33]. The unique mesopore structure of Cu_2O nanocubes on the SPCE surface can help to better immobilize and increase loading of biomolecules. Moreover, it would bring about an efficient retaining of the activity and increasing the sensitivity of the electrochemical analyses in the designed biosensor. These advantages make Cu_2O NCs a suitable choice in designing electrochemical biosensors. In addition, as sensitive immunological diagnostic method for SARS-CoV-2, the designed nanobiodevice requires no sample pretreatment or labeling. In this sense, the disadvantages of the labeling process include high cost, complexity, and changing the biomolecule's activity [33].

The selection of antibody immobilization method has become one of the key points in the fabrication of immunosensor. The immobilized antibodies with well-defined orientation can greatly increase antigen-binding capacity and improve the function of the detection system [34]. Staphylococcal protein A (ProtA) is considerably significant as a strong immunological instrument and has long been utilized because of its ability to strongly bind to the Fc region of IgG antibodies [35–37]. Recombinant anti-SARS-CoV-2 spike protein antibody is a human IgG recombinant version which recognizes the SARS-CoV-2 spike protein, the causative agent of SARS-CoV-2. Therefore, the antibody will be positioned on the ProtA surface with a suitable orientation to bind to the antigen and interact with specific antigens.

Herein, in order to detect spike protein, we suggest a novel ultrasensitive electroanalytical nanobiodevice made by using ProtA/Cu_2O NC–modified SPCE as substrate for the ordered orientation of IgG antibodies as a specific receptor. Cyclic voltammetry (CV) and electrochemical impedance spectroscopy (EIS) were applied to investigate the proposed biodevice and analyze the spike protein using $[Fe(CN)_6]^{4-/3-}$ as the redox probe. This nanobiodevice requires no sample pretreatment or labeling and because of the use of SPCE and also due to their small size, it is not necessary to have a large population and volume of the samples. Accordingly, a low-cost and miniaturized sensor can be embedded, allowing the possibility of an in situ testing and on-site screening of samples. Moreover, the detection performance of the developed nanobiodevice

was tested in different artificial sample matrices such as saliva, artificial nasal, and UTM, and also real patients and healthy people samples where the results are already confirmed using the standard PCR procedure.

Experimental section

Materials

Spike protein antigen (76.5 kDa) and antibodies were purchased from Cusabio Company (https://www.cusabio.com). Disodium hydrogen phosphate (Na_2HPO_4), monosodium dihydrogen phosphate (NaH_2PO_4), cupric chloride dihydrate ($CuCl_2{\cdot}2H_2O$), sodium hydroxide (NaOH), and all other reagents were purchased from Sigma-Aldrich and Merck Co. LLC (USA) and, then, used without further purification. In order to prepare the phosphate buffer (PB), 0.1 M Na_2HPO_4 and NaH_2PO_4 were applied. Besides, in our experiments, we applied a solution which contained 5 mM $K_3Fe(CN)_6/K_4Fe(CN)_6$ at a ratio of 1:1 and 0.1 M KCl as a redox probe. In this regard, the deionized water was used for the solutions. It is worth mentioning that the room temperature 25 ± 0.5 °C was used in order to perform the experiments.

Apparatus and procedures

EIS and CV were used to record electrochemical data. In this regard, μ-AUTOLAB electrochemical system type III and FRA2 board computer, which were controlled by potentiostat/galvanostat (Eco-Chemio, Switzerland) and driven with NOVA software, were applied. We used a SPCE with 2 mm in diameter from DropSens (Spain) as a planar three-electrode which was based on a carbon counter electrode, a silver pseudo-reference electrode, and a graphite working electrode. We executed the EIS analysis within the frequency range of 0.1–100 kHz with 5 mV amplitude and with a bias potential of 0.25 V. In order to measure the pH, a Metrohm pH meter (model 780 pH/mV meters) was applied. Moreover, morphological, structural, and chemical analyses of the samples were performed applying a FESEM (TESCAN, Mira III LMU, Czech Republic), equipped with an EDS probe.

Preparation of solid Cu_2O NCs

Conventional Cu_2O NCs were prepared following the previous literature reports [26]. This section is presented in Electronic Supplementary Material.

Construction of the nanobiodevice

The fabrication procedure of the nanobiodevice is shown in Scheme 1. Before using the SPCE, in order to electrochemically activate its surface, 10 μL of H_2SO_4 (2 M) was carefully dropped on the SPCE surface, and, then, we applied a voltage of 1.5 V during 150 s. Afterwards, the clean SPCE was washed with distilled water and dried under N_2 gas. Subsequently, 1 mg of the prepared Cu_2O NC powder was dispersed into 1 mL of distilled water for 30 min and 10 μL of it was drop-coated on the surface of the electrode. Subsequently, the solvent was allowed to evaporate at room temperature. The modified electrode is hereafter denoted as Cu_2O NC/SPCE. Eventually, 10 μL of ProtA (10 mg mL^{-1}) in PB was dropped onto the surface of the Cu_2O NC/SPCE for 45 min in order to the ProtA molecules immobilized onto the Cu_2O NC/SPCE surface. In the next step, 10 μL of IgG antibody (30 mg mL^{-1}) in PB was casted onto the BSA/ProtA/Cu_2O NC/SPCE surface for 35 min in order to bind onto the electrode surface in an ordered orientation via ProtA. Afterwards, in order to block the available active sites and unspecific interaction, 10 μL of BSA (1%) solution was dropped onto the modified electrode.

After each step, PB was used to thoroughly rinse the electrode with the aim of removing the unbonded molecules. Moreover, it was dried under N_2 gas, and, then, the obtained IgG/BSA/ProtA/Cu_2O NCs/SPCE, as a biodevice, was directly applied for the detection experiments or stored at 4 °C to later use.

Analysis protocol

The samples were analyzed by EIS technique as the measuring technique. Besides, in order to investigate their repeatability, each sample was tested three times. For different artificial sample matrices, various concentrations of spike protein were added to these samples, and, then, 6 μL of each solution, containing different concentrations of spike protein, was separately drooped on the nanobiodevice independent from the others. Besides, the standard addition method was adopted for this purpose, and, finally, recoveries of different concentrations of spike protein were also investigated.

The real patients and healthy individual samples where the results are already confirmed using the standard PCR procedure were provided from a clinical laboratory. The nasopharyngeal swab samples in UTM and saliva were inactivated by being heated at 100 °C for 10 min and were stored in the freezer for further use. The samples were diluted ten times with PB and, then, tested by nanobiodevice.

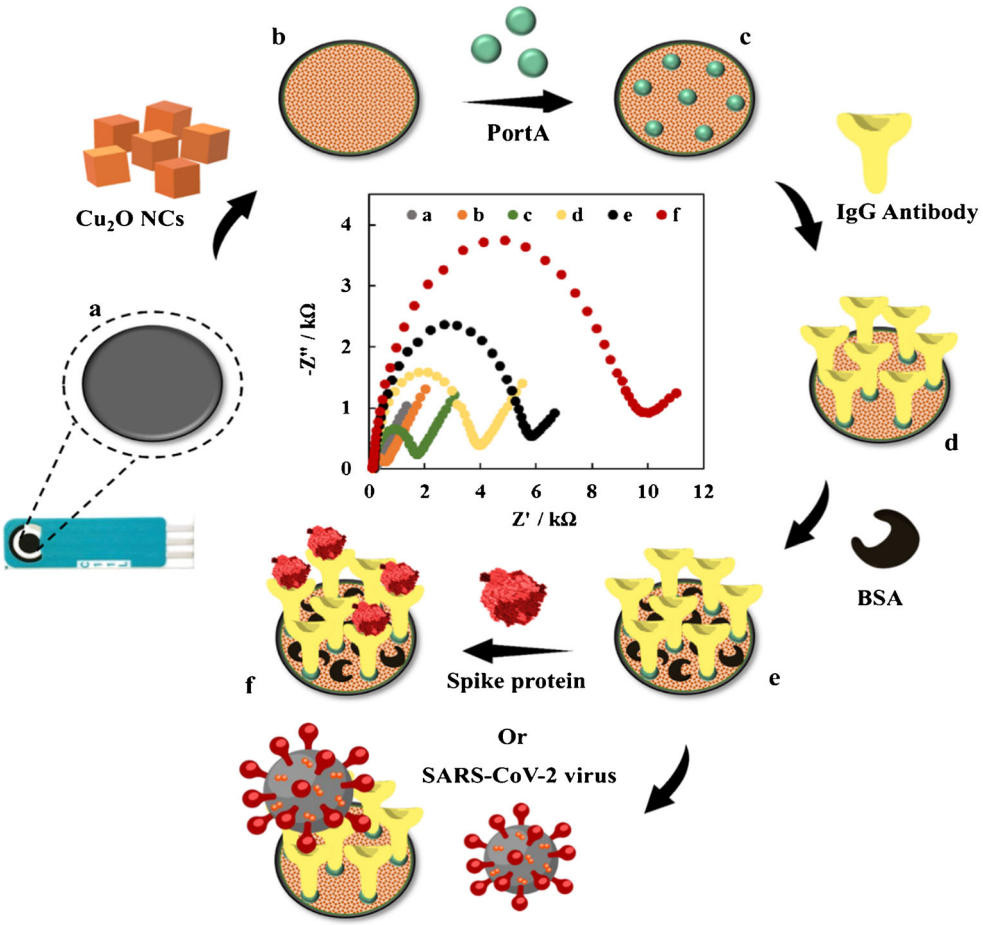

Scheme 1 Schematic of the step-by-step preparation of nanobiodevice

Results and discussion

Characterization of the synthesized Cu_2O NCs

The results about the characterization of Cu_2O NCs are available in the Electronic Supplementary Material (Fig. 1S, Fig. 2S, and Fig. 3S).

Study the characterization of the biodevice

CV and EIS were applied with the aim of demonstrating the stepwise fabrication process of the nanobiodevice (Fig. 1a, b). The EIS can be regarded as an applicable method used in obtaining electrical information in a broad range of frequency and monitoring the modified electrode traits [38]. Evidently, there are two portions in the Nyquist plot: the electron transfer process is indicated by the semicircle portion at higher frequencies, while, at lower frequencies, the electron diffusion process is represented by the linear part. As corresponding to the diameter of the semicircle, the R_{ct} is an important parameter. Therefore, in order to investigate the surface properties during the fabrication process of the biodevice, the variations in the R_{ct} amounts for different modified electrodes at each stage were selected. As seen in Fig. 1a, the R_{ct} value of the bare SPCE was the lowest, illustrating the fact that the electroactive ions of $[Fe(CN)_6]^{3-/4-}$ are rapidly transported to the electrode interface (curve a, $R_{ct} = 0.17$ kΩ). Evidently, as a result of pouring some of the Cu_2O NCs on the SPCE, we witnessed an increase in the R_{ct} (curve b, $R_{ct} = 0.8$ kΩ). Since the Cu_2O NCs were regarded as a semiconductor and were formed of metal oxide with the negative partial charge, the resistance increased due to repulsion between the Cu_2O NCs and the anion redox probe, indicating the good attachment of this nanocomposite. The mesopore structure of Cu_2O NCs can make a suitable substrate in order to increase the loading of ProtA onto the surface of SPCE.

When ProtA is immobilized onto the Cu_2O NC/SPCE surface, we witnessed the enlargement of the semicircle diameter and an increase in R_{ct} to 0.4 kΩ. This increase in the R_{ct} can be because of the steric/conformational restrictions created on the electrode surface via the bulky ProtA molecules which retard the redox probe to reach the surface (curve c, $R_{ct} = 1.8$ kΩ). Similarly, an increase in R_{ct} was observed after IgG antibody was bound to ProtA/Cu_2O NC/SPCE electrode surface via the Fc portion. In this sense, the electron transfer of $[Fe(CN)_6]^{3-/4-}$ with the electrode was made more difficult by the binding

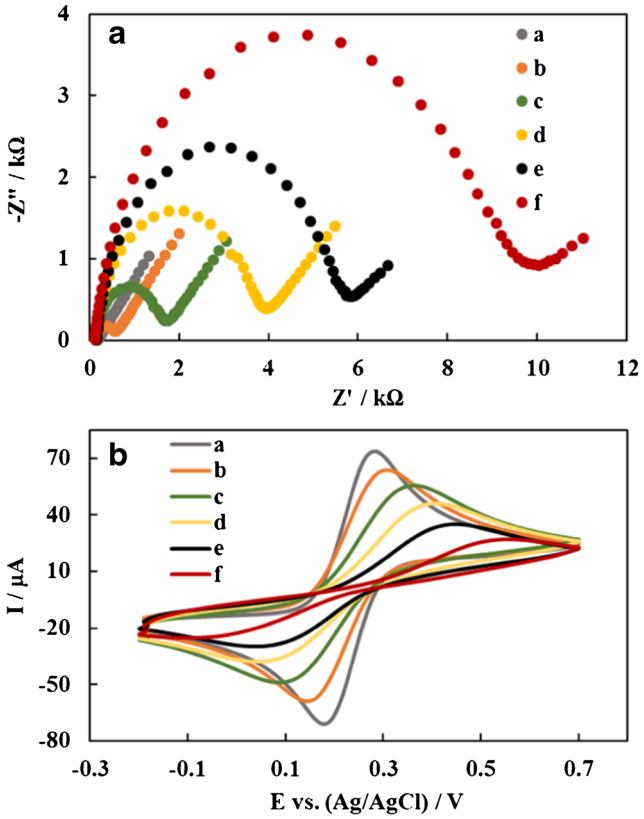

Fig. 1 EIS (**a**) and CV (**b**) characterization of different modified electrodes SPCE (a), Cu_2O NC/SPCE (b), ProtA/Cu_2O NC/SPCE (c), IgG/ProtA/Cu_2O NC/SPCE (d), BSA/IgG/ProtA/Cu_2O NC/SPCE (e), and spike protein/BSA/IgG/ProtA/Cu_2O NC/SPCE (f)

antibody (curve d, $R_{ct} = 3.94$ kΩ). Subsequently, when the BSA blocked the nonspecific active sites on the electrode surface, a further increase in R_{ct} was observed (curve e, $R_{ct} = 5.9$ kΩ). In the last step, by incubating 100 pg mL^{-1} of the spike protein as a target onto the BSA/IgG/ProtA/Cu_2O NC/SPCE, R_{ct} increased representing a successful connection of spike protein to IgG (curve f, $R_{ct} = 10$ kΩ).

To further verify the assembling state of the modified electrode, the CV technique was also employed (Fig. 1b). A well-defined sharp redox peak for the reduction of the $[Fe(CN)_6]^{3-/4-}$ was obtained at the bare carbon electrode (curve a, ΔE = 12 mV). By modifying the SPCE with Cu_2O NCs, the peak current decreased due to the repulsion between the probe anions and the negatively charged Cu_2O NCs (curve b, $\Delta E = 16$ mV). By attaching the ProtA onto the Cu_2O NC/SPCE, a noticeable decrease of the current along with the increment of the ΔE value occurred (curve c, $\Delta E = 25$ mV), and similarly, a decrease in the current was observed when IgG and BSA were incubated on the electrode surface (curve d, ΔE = 31 mV, and curve e, ΔE = 40 mV). This electrochemical change may be attributed to the successful attachment of each layer onto the electrode surface, and, consequently, the resulted steric/conformational restrictions would lead to inhabitation of the electron transfer between $[Fe(CN)_6]^{3-/4-}$ and the surface of the modified electrode. As expected, when spike protein was dropped onto the nanobiodevice surface, more steric/conformational restrictions and, thereby, a significant decrease in the CV response were observed (curve f, $\Delta E = 52$ mV). The obtained results of both techniques were in agreement confirming the fact that the nanobiodevice is successfully prepared and is also useful in spike protein measuring.

Optimization study of the experiment

In order to obtain a high and stable electrochemical response from immunosensor, optimization of some experimental parameters is necessary. Respective text and figures on optimizations are given in the Electronic Supplementary Material (Fig. 3S). In short, the following experimental conditions were found to give the best results: optimal concentration of ProtA: 10 μg mL^{-1}; best incubation time of ProtA: 45 min; optimal concentration of IgG antibody: 30 μg mL^{-1}; best incubation time of IgG antibody: 35 min; and best incubation time of spike protein: 20 min.

Performance study of the biodevice

In order to evaluate SARS-CoV-2 nanobiodevice performance, the nanobiodevice dynamic response to spike protein was evaluated under the optimal conditions using the EIS technique. Figure 2a illustrates the Nyquist plots for the nanobiodevice obtained from different spike protein concentrations. As seen in Fig. 2a, one can observe a gradual increase in the diameter of the semicircle in the Nyquist plots specifically when the concentration of spike protein increased. In this sense, it can indicate the inhibition effects of spike protein on the electron transfer between redox probe and the electrode surface. This means that the interfacial properties can be altered even by little changes in the surface induced by specific binding of IgG antibody with spike protein. The R_{ct} value as the response of the sensor increased proportional to the logarithm of the different concentrations of the spike protein in ranges from 0.25 fg mL^{-1} to 1 μg mL^{-1} as the linear regression equation is $\Delta R_{ct} = 7.5688 \log C$ (fg mL^{-1}) + 5.9414 ($R^2 = 0.9933$) with a LOD of 0.04 fg mL^{-1} estimated by 3σ, where σ is the relative standard deviation of a blank solution ($n = 5$). In other words, the LOD of the designed nanobiodevice was greatly lower than that of the ELISA platform indicating the good sensitivity of our sensor [39]. In this regard, it can be attributed to the Cu_2O NC–modified electrodes resulting in an increase in the electrode surface area and a successful immobilization of IgG antibody on the electrode surface in an ordered orientation through ProtA molecules, which are stabilized on the Cu_2O NC–modified electrode, as well as the high sensitivity of the EIS technique. The proposed electrochemical sensor has the following advantages: being user-friendly and less costly than quantitative real-time RT-

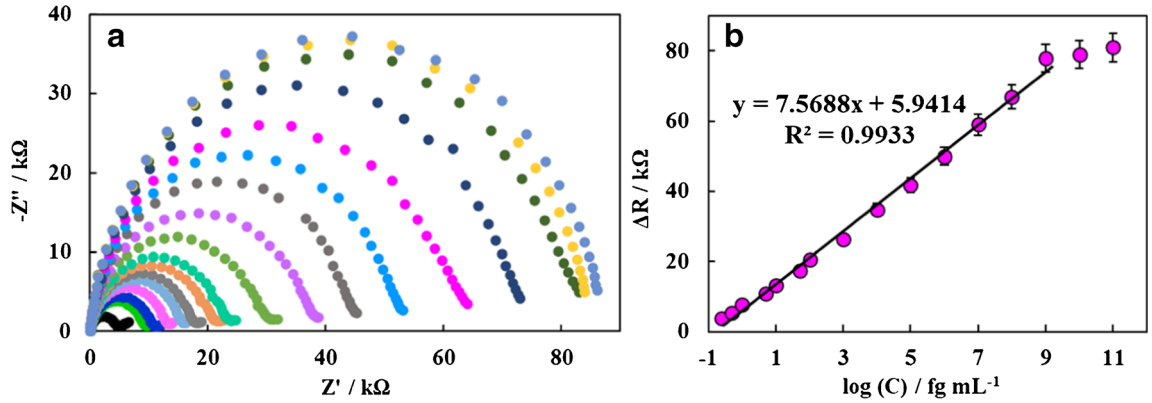

Fig. 2 EIS responses of the designed biodevice after incubation with different spike proteins with concentrations of 0, 0.25 fg mL^{-1}, 0.5 fg mL^{-1}, 1 fg mL^{-1}, 5 fg mL^{-1}, 10 fg mL^{-1}, 50 fg mL^{-1}, 100 fg mL^{-1}, 1 pg mL^{-1}, 10 pg mL^{-1}, 100 pg mL^{-1}, 1 ng mL^{-1}, 10 ng mL^{-1}, 100 ng mL^{-1}, and 1 μg mL^{-1} ($n = 3$). Calibration curve of ΔR_{ct} vs log $C_{spike\ protein}$ (fg mL^{-1})

PCR and having high sensitivity of the EIS technique. As a result, it will become more suitable in areas with limited resources and expertise. Consequently, this method can excellently detect SARS-CoV-2 due to the following advantages: high sensitivity and fast response along with the low cost and capability of miniaturization. A comparison of the proposed nanobiodevice performance with some other sensor for SARS-CoV-2 is summarized in Table S1. From Table S1, it was found that the LOD and assay reaction time of the nanobiodevice are similar or better than the reported methods.

Selectivity, stability, and reproducibility of the method

Practically, a sensor should be not only sensitive but also specific. Therefore, it is very important to confirm the selectivity of the designed nanobiodevice over the possible interference in order to avoid false identification. In order to understand that the observed behavior of the nanobiodevice was not due to nanobiodevice degradation or nonspecific binding, the response of the nanobiodevice was studied against other potentially unrelated interfering species such as influenza viruses 1 and 2 with more 10^3-fold concentration than the 1 pg mL^{-1} of spike protein. As can be seen in Fig. 3a, by incubating spike protein, a well-defined response was observed at the designed nanobiodevice, whereas no important response in the presence of the probable interfering species was detected. This behavior is consistent with what previously stated: the binding event between the sensing interface and the target would be under a selective recognition between them, not on nonspecific adsorption. Moreover, when the nanobiodevice surface is blocked with BSA, it results in preventing interference with other disturbing species.

Another attractive feature of this nanobiodevice was its high operational stability for spike protein detection. In this sense, CVs of the 2nd and 100th cycles applied on the nanobiodevice were recorded in the electrolyte solution and in the presence of 10 pg mL^{-1} of the spike protein at a scan rate of 100 mV s^{-1} (Fig. 3b). According to the results, the suggested platform based on the Cu_2O NCs and the loaded ProtA and IgG antibody can be greatly attached to the surface of electrode. In this regard, it would indicate high stability of the nanobiodevice, so that the peak separation was remained unchanged with only 3% reduction in peak current intensity. Moreover, the long-term stability of the designed nanobiodevice was evaluated on a 14-day period by storing it at 4 °C. Besides, only around 3% change in the response was observed, indicative of good stability of the assay.

Furthermore, the reproducibility of the nanobiodevice was also evaluated. Five modified SPCEs were prepared and their EIS measuring experiments for 100 pg mL^{-1} of spike protein were performed. The nanobiodevice displayed response to relative standard deviation (RSD) of 3.1% indicating a very good reproducibility of the nanobiodevice (Fig. 3c). Moreover, for five repeated measurements of 100 pg mL^{-1} of spike protein, the repeatability of the sensor was evaluated. The RSD value of 1.7% was obtained; this evidence confirms that the designed aptasensor has excellent repeatability (data not shown).

Moreover, the control electrode was assayed with the ProtA and BSA-modified electrode without IgG antibody conjugation. No significant response was obtained after incubating different target concentrations for the control electrodes which indicated that there would be no nonspecific adsorption on the nanobiodevice and that the IgG antibody is necessary for specific binding with the spike protein (data not shown).

The above satisfactory results verify the potential application of the nanobiodevice in ultrasensitive and specific analysis of the spike protein.

Real sample analysis

In order to assay the feasibility of using the designed nanobiodevice with the aim of detecting the virus in

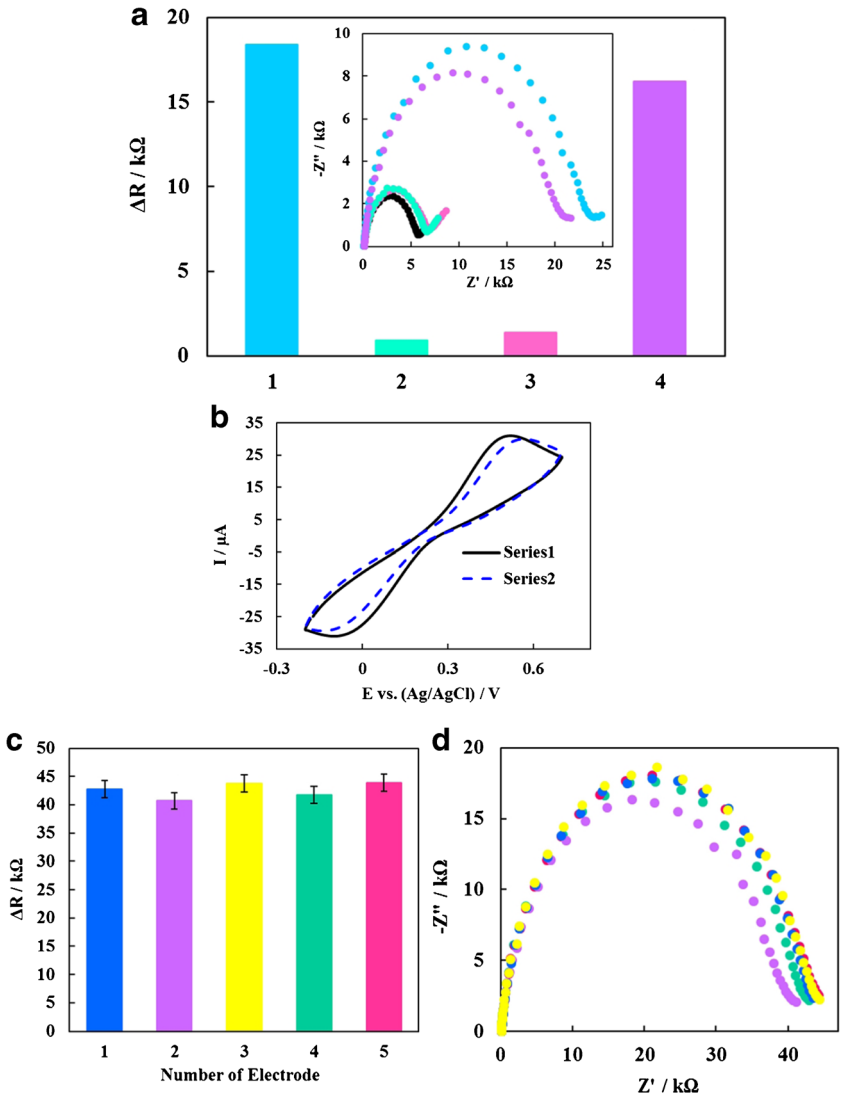

Fig. 3 **a** EIS response and histogram of the biodevice after incubation with spike protein (1) and some off-target species such as influenza A (2) and B (3) antigen and a mixture (4) of them. **b** The recorded CVs of the 2th and 100th cycles related to the spike protein/BSA/IgG/ProtA/Cu_2O NC/SPCE in electrolyte solution with scan rate of 100 mV s^{-1}. **c** Reproducibility investigation of the aptasensor for 100 pg mL^{-1} of spike protein on the five different modified electrodes and **d** EIS response of each electrode

biological fluids, saliva and artificial nasal samples spiked with spike protein were analyzed. Most notably, considering that in the clinic, SARS-CoV-2 diagnosis was performed applying nasopharyngeal swabs suspended in UTM due to the fact that it contained different reagents which might affect the nanobiodevice performance, i.e., Hank's balanced salts and BSA. Hence, the nanobiodevice's response to spike protein in UTM was also investigated. As can be seen in Table 1, the spiked samples which were evaluated in each case illustrated high recovery percentages ranging from 97 to 103%. Besides, the RSDs were also found to be 3.1% indicating good precision of the assay. Standard addition method was also applied to UTM samples including spike protein. Its calibration equation is found to be $\Delta R_{ct} = 7.584 \log C\ (\text{fg mL}^{-1}) + 5.24$ (R^2 = 0.9978). The slopes of both methods are almost identical. Hence, spike protein recognition is accomplished without interference.

Moreover, for the feasibility of nanobiodevice in the detection of SARS-CoV-2 virus in biological samples, the detection performance of nanobiodevice was tested using clinical samples. Additionally, the obtained results are summarized in

Table 1 Measurement of spike protein in real samples with proposed nanobiodevice

Samples	Added	Founded	Recovery (%)	RSD (%)
Saliva	10 fg mL^{-1}	9.8 fg mL^{-1}	98	2.9
	10 ng mL^{-1}	10.2 ng mL^{-1}	102	2.8
Artificial nasal	10 fg mL^{-1}	10.3 fg mL^{-1}	103	3.1
	10 ng mL^{-1}	9.7 ng mL^{-1}	97	2.9
UTM	10 fg mL^{-1}	10.2 fg mL^{-1}	102	2.8
	10 ng mL^{-1}	9.9 ng mL^{-1}	99	3.0

Each sample is measured three times

Table 2 Detection of SARS-CoV-2 virus in clinical samples with proposed nanobiodevice

	UTM samples		Saliva samples	
Patients	Nanobiodevice test	PCR test	Nanobiodevice test	PCR test
#1	+	+	+	+
#2	+	+	+	+
#3	+	+	+	+
#4	+	+	+	+
#5	+	+	+	+
#6	+	+	+	+
#7	+	+	+	+
#8	+	+	+	+
#9	−	−	−	−
#10	−	−	−	−
#11	−	−	−	−
#12	−	−	−	−
#13	−	−	−	−
#14	−	−	−	−
#15	−	−	−	−
#16	−	−	−	−

Table 2 and compared with the PCR test. The results showed possible application of the nanobiodevice to detect spike protein antigens and SARS-CoV-2 virus in real samples, without any preparation or preprocessing, and exhibited great promise as a reliable nanotool for the detection of spike protein antigen and SARS-CoV-2 virus in real biological samples.

Conclusion

Herein, we have offered an electrochemical nanobiodevice which was applied for rapid screening of people suspicious to SARS-CoV-2 with the aim of facilitating the point-of-care diagnosis. In this sense, the disposable SPCEs were modified with Cu_2O NCs, and, then, the ProtA layer was used to immobilize the IgG antibody, as a receptor element, in the regular direction. This sensor was able to be used in clinical samples to detect the SARS-CoV-2 virus in less than 20 min, without any cross-reactivity when tested with influenza viruses 1 and 2. The results rely on some key features: (1) the Cu_2O NCs provide a good substrate for ProtA stabilization and also can create more active sites for ProtA immobilization on the electrode surface; (2) great amplified sensitivity and selectivity were achieved by loading large amounts of the ProtA and following that the IgG, in an ordered orientation through ProtA as a spike protein–specific antibody, led to a greater formation of the spike protein-IgG complex and enhanced the nanobiodevice response; (3) the use of BSA blocks the available active sites, prevents nonspecific adsorption, and provides a specific sensing interface which prevents interference with other disturbing species. The obtained results demonstrate that the fabricated nanobiodevice is capable of being used as a model of the promising clinical tool which can be used in the early-stage screening of SARS-CoV-2 with satisfactory results.

Supplementary Information The online version contains supplementary material available at https://doi.org/10.1007/s00604-021-04762-9.

Compliance with ethical standards

All experimental protocols were approved by the Experimentation Ethics Committee of Ilam University of Medical Sciences (Code: IR. MEDILAM. REC.1399.210). The clinical samples were provided from a local clinical laboratory. Informed consent was obtained from all participants included in the study

Conflict of interest The authors declare that they have no competing interests.

References

1. Novel CPERE (2020) The epidemiological characteristics of an outbreak of 2019 novel coronavirus diseases (COVID-19) in China. Zhonghua liu xing bing xue za zhi= Zhonghua liuxingbingxue zazhi 41:145
2. Layqah LA, Eissa S (2019) An electrochemical immunosensor for the corona virus associated with the Middle East respiratory syndrome using an array of gold nanoparticle-modified carbon electrodes. Microchim Acta 186:1–10
3. Yang X, Yu Y, Xu J, et al (2020) Clinical course and outcomes of critically ill patients with SARS-CoV-2 pneumonia in Wuhan, China: a single-centered, retrospective, observational study. Lancet Respir Med
4. Antiochia R (2020) Nanobiosensors as new diagnostic tools for SARS, MERS and COVID-19: from past to perspectives. Microchim Acta 187:1–13
5. Fauci AS. Covid-19—navigating the uncharted, editorial published on February 28, 2020, at. NEJM org
6. Vogel G (2020) New blood tests for antibodies could show true scale of coronavirus pandemic. Sci Mag AAAS, DC, USA
7. Chan JF-W, Yip CC-Y, To KK-W et al (2020) Improved molecular diagnosis of COVID-19 by the novel, highly sensitive and specific COVID-19-RdRp/Hel real-time reverse transcription-PCR assay validated in vitro and with clinical specimens. J Clin Microbiol 58
8. Chu DKW, Pan Y, Cheng SMS, Hui KPY, Krishnan P, Liu Y, Ng DYM, Wan CKC, Yang P, Wang Q, Peiris M, Poon LLM (2020) Molecular diagnosis of a novel coronavirus (2019-nCoV) causing an outbreak of pneumonia. Clin Chem 66:549–555
9. Morales-Narváez E, Dincer C (2020) The impact of biosensing in a pandemic outbreak: COVID-19. Biosens Bioelectron 112274
10. Raouafi A, Sánchez A, Raouafi N, Villalonga R (2019) Electrochemical aptamer-based bioplatform for ultrasensitive detection of prostate specific antigen. Sensors Actuators B Chem 297:126762

11. Villalonga A, Pérez-Calabuig AM, Villalonga R (2020) Electrochemical biosensors based on nucleic acid aptamers. Anal Bioanal Chem 1–18
12. Singh R, Mukherjee MD, Sumana G et al (2014) Biosensors for pathogen detection: a smart approach towards clinical diagnosis. Sensors Actuators B Chem 197:385–404
13. Medetalibeyoglu H, Kotan G, Atar N, Yola ML (2020) A novel sandwich-type SERS immunosensor for selective and sensitive carcinoembryonic antigen (CEA) detection. Anal Chim Acta 1139:100–110
14. Roushani M, Rahmati Z, Golchin M et al (2020) Electrochemical immunosensor for determination of Staphylococcus aureus bacteria by IgY immobilized on glassy carbon electrode with electrodeposited gold nanoparticles. Microchim Acta 187:1–8
15. Medetalibeyoglu H, Kotan G, Atar N, Yola ML (2020) A novel and ultrasensitive sandwich-type electrochemical immunosensor based on delaminated MXene@ AuNPs as signal amplification for prostate specific antigen (PSA) detection and immunosensor validation. Talanta 220:121403
16. Medetalibeyoglu H, Beytur M, Akyıldırım O, Atar N, Yola ML (2020) Validated electrochemical immunosensor for ultrasensitive procalcitonin detection: carbon electrode modified with gold nanoparticles functionalized sulfur doped MXene as sensor platform and carboxylated graphitic carbon nitride as signal amplification. Sensors Actuators B Chem 319:128195
17. Yola ML, Atar N (2020) Amperometric galectin-3 immunosensor-based gold nanoparticle-functionalized graphitic carbon nitride nanosheets and core–shell Ti-MOF@ COFs composites. Nanoscale 12:19824–19832
18. Seo G, Lee G, Kim MJ, Baek SH, Choi M, Ku KB, Lee CS, Jun S, Park D, Kim HG, Kim SJ, Lee JO, Kim BT, Park EC, Kim SI (2020) Rapid detection of COVID-19 causative virus (SARS-CoV-2) in human nasopharyngeal swab specimens using field-effect transistor-based biosensor. ACS Nano 14:5135–5142
19. Vadlamani BS, Uppal T, Verma SC, Misra M (2020) Functionalized TiO2 nanotube-based electrochemical biosensor for rapid detection of SARS-CoV-2. Sensors 20:5871
20. Rashed MZ, Kopechek JA, Priddy et al (2021) Rapid detection of SARS-CoV-2 antibodies using electrochemical impedance-based detector. Biosens Bioelectron 171:112709
21. Fabiani L, Saroglia M, Galatà G, de Santis R, Fillo S, Luca V, Faggioni G, D'Amore N, Regalbuto E, Salvatori P, Terova G, Moscone D, Lista F, Arduini F (2021) Magnetic beads combined with carbon black-based screen-printed electrodes for COVID-19: a reliable and miniaturized electrochemical immunosensor for SARS-CoV-2 detection in saliva. Biosens Bioelectron 171:112686
22. Rahmati Z, Roushani M, Hosseini H Three-dimensional NiCo2O4 nanowires encapsulated in nitrogen-doped carbon networks as a high-performance aptamer stabilizer for impedimetric ultrasensitive detection of hepatitis C virus core antigen. Surfaces Interfaces 22: 100813
23. Valipour A, Roushani M (2017) Using silver nanoparticle and thiol graphene quantum dots nanocomposite as a substratum to load antibody for detection of hepatitis C virus core antigen: electrochemical oxidation of riboflavin was used as redox probe. Biosens Bioelectron 89:946–951
24. Roushani M, Shahdost-fard F (2018) Impedimetric detection of cocaine by using an aptamer attached to a screen printed electrode modified with a dendrimer/silver nanoparticle nanocomposite. Microchim Acta 185:214
25. Arduini F, Amine A, Majorani C, di Giorgio F, de Felicis D, Cataldo F, Moscone D, Palleschi G (2010) High performance electrochemical sensor based on modified screen-printed electrodes with cost-effective dispersion of nanostructured carbon black. Electrochem Commun 12:346–350
26. Caratelli V, Ciampaglia A, Guiducci J et al (2020) Precision medicine in Alzheimer's disease: an origami paper-based electrochemical device for cholinesterase inhibitors. Biosens Bioelectron 112411
27. Shahdost-fard F, Roushani M (2020) Architecting of a biodevice based on a screen-printed carbon electrode modified with the NiONP nanolayer and aptamer in BCM-7 detection. Colloids Surf B: Biointerfaces 110932
28. Xu W, Yi H, Yuan Y, Jing P, Chai Y, Yuan R, Wilson GS (2015) An electrochemical aptasensor for thrombin using synergetic catalysis of enzyme and porous Au@ Pd core–shell nanostructures for signal amplification. Biosens Bioelectron 64:423–428
29. Kurbanoglu S, Ozkan SA, Merkoci A (2017) Nanomaterials-based enzyme electrochemical biosensors operating through inhibition for biosensing applications. Biosens Bioelectron 89:886–898
30. Liu M, Liu R, Chen W (2013) Graphene wrapped Cu2O nanocubes: non-enzymatic electrochemical sensors for the detection of glucose and hydrogen peroxide with enhanced stability. Biosens Bioelectron 45:206–212
31. Espro C, Marini S, Giusi D et al (2020) Non-enzymatic screen printed sensor based on Cu2O nanocubes for glucose determination in bio-fermentation processes. J Electroanal Chem 114354
32. Zhang Z, Zhang S, Liu S, Wang M, Fu G, He L, Yang Y, Fang S (2015) Electrochemical aptasensor based on one-step synthesis of Cu2O@ aptamer nanospheres for sensitive thrombin detection. Sensors Actuators B Chem 220:184–191
33. Syahir A, Usui K, Tomizaki K, Kajikawa K, Mihara H (2015) Label and label-free detection techniques for protein microarrays. Microarrays 4:228–244
34. Zhou J, Du L, Zou L et al (2014) An ultrasensitive electrochemical immunosensor for carcinoembryonic antigen detection based on staphylococcal protein A—Au nanoparticle modified gold electrode. Sensors Actuators B Chem 197:220–227
35. Zuo B, Li S, Guo Z, Zhang J, Chen C (2004) Piezoelectric immunosensor for SARS-associated coronavirus in sputum. Anal Chem 76:3536–3540
36. Sasso EH, Silverman GJ, Mannik M (1991) Human IgA and IgG F (ab') 2 that bind to staphylococcal protein A belong to the VHIII subgroup. J Immunol 147:1877–1883
37. Zhang DF, Zhang H, Guo L, Zheng K, Han XD, Zhang Z (2009) Delicate control of crystallographic facet-oriented Cu_2O nanocrystals and the correlated adsorption ability. J Mater Chem 19:5220–5225
38. Roushani M, Rahmati Z, Hoseini SJ, Fath RH (2019) Impedimetric ultrasensitive detection of chloramphenicol based on aptamer MIP using a glassy carbon electrode modified by 3-ampy-RGO and silver nanoparticle. Colloids Surf B: Biointerfaces 183:110451
39. Sunwoo HH, Palaniyappan A, Ganguly A, Bhatnagar PK, Das D, El-Kadi AO, Suresh MR (2013) Quantitative and sensitive detection of the SARS-CoV spike protein using bispecific monoclonal antibody-based enzyme-linked immunoassay. J Virol Methods 187:72–78